HHS Public Access

Author manuscript

Nanoscale. Author manuscript; available in PMC 2016 October 28.

Published in final edited form as:

Nanoscale. 2015 October 28; 7(40): 17139–17147. doi:10.1039/c5nr03399c.

Van der Waals Force-Induced Loading of Proangiogenic Nanoparticles on Microbubbles for Enhanced Neovascularization

Jinrong Chen[a], **Min Kyung Lee**[a], **Sanjay Misra**[b], and **Hyunjoon Kong**[a,c,d]

[a]Department of Chemical and Biomolecular Engineering, University of Illinois at Urbana-Champaign, 600 South Mathews Avenue, Urbana, IL 61801, USA

[b]Department of Radiology, Mayo Clinic, 201 1st Street SW, Rochester, MN 55902, USA

[c]Institute for Genomic Biology, University of Illinois at Urbana-Champaign, 1206 West Gregory Drive, Urbana, IL 61801, USA

[d]Department of Chemical Engineering, Soongshil University, Seoul, South Korea

Abstract

Nanoparticles emerged as carriers of promising diagnostic and therapeutic molecules due to their unique size, injectability, and potentials to sustainably release molecular cargos. However, with local injection of particles into target tissue, the significant particle loss caused by external biomechanical forces is a grand challenge yet to be resolved up to date. We hypothesized that nanoparticles associated with tissue-adherent microbubbles in a form of core-shell particles due to van der Waals attractive force would stably remain on an implanted site and significantly increase therapeutic efficacy of drug cargos. To examine this hypothesis, we used 100 nm-diameter nanoparticles made of poly(lactide-co-glycolic acid) (PLGA) as a model nanoparticle and 50 μm-diameter microbubbles made of poly(2-hydroxyethyl aspartamide) (PHEA) grafted with octadecyl chains, PHEA-g-C_{18}, as a model microbubble. Simple mixing of PLGA nanoparticles and PHEA-g-C_{18} microbubbles resulted in the core-shell particles. Following implantation, the PHEA-g-C_{18} microbubble acted as a glue to minimize displacement of PLGA nanoparticles, because of association between octadecyl chains on PHEA-g-C_{18} and epithelium of tissue. As a consequence, the core-shell particles prepared with Angiopoietin-1(Ang1)-encapsulated PLGA nanoparticles significantly promoted vascularization in the implanted tissue. Overall, the results of this study provide a simple but advanced strategy for improving therapeutic efficacy of drug-carrying nanoparticles without altering their surface chemistry and potential.

1. INTRODUCTION

Nanoparticles, capable of loading and also sustainably releasing diagnostic and therapeutic molecules of interests, have been extensively studied to improve the quality of molecular cargos via non-invasive injection.[1–5] However, nanoparticles particularly delivered through local injection are readily displaced from the implanted site, because the external biomechanical force increases drifting velocity of particles.[6–8] As a consequence, a larger

*To whom correspondence should be addressed: hjkong06@illinois.edu.

dosage of drug is required to attain the desired therapeutic efficacy, thus reducing advantages that can be achieved with the use of nanoparticles. Therefore, it is crucial to devise a method to make nanoparticles remain in injected tissue over a desired treatment period following non-invasive administration.

Recently, certain efforts were made to improve the retention level of nanoparticles following injection. For example, drug-loaded nanoparticles were embedded in an injectable hydrogel such the gel can prevent displacement of nanoparticles.[9,10] However, this approach may reduce the release rate of molecular cargos in the nanoparticles, because the gel matrix acts as a physical barrier to limit molecule release, specifically when drug molecules and gel-forming polymers electrostatically attract to each other.[9] Alternatively, surface potential of nanoparticles was engineered to induce electrostatic attraction between nanoparticles, so nanoparticles form an interconnected colloidal gel following injection.[10] However, again, surface potential of nanoparticles may negatively influence drug release rate via uncontrolled electrostatic interaction. It will be desirable to control the nanoparticle retention without altering chemistry and electrical charge of particle surfaces.

To this end, we hypothesized that nanoparticles associated with tissue adherent microbubbles in a form of a core-shell-like construct due to van der Waals attractive force would stably remain on an implanted site and significantly increase therapeutic efficacy of drug cargos. The microbubble glue would limit the increase of drifting velocity of nanoparticles caused by the external biomechanical force without influencing drug release profile of nanoparticles. To examine this hypothesis, we used microbubbles with an average diameter of about 50 μm, formed from self-assembly of alkylated poly(2-hydroxyethyl aspartamide) (PHEA-g-C_{18}) as a model of sacrificial microbubbles. The alkyl groups of PHEA do not only associate air molecules to form bubbles but also bind with tissue epithelium.[11] The poly(lactic-co-glycolic acid) (PLGA) nanoparticles with an average diameter of about 100 nm was used as a model of drug-carrying nanoparticles. The difference between the diameters of microbubbles and nanoparticles by two orders of magnitude can induce significantly higher van der Waals attraction between microbubble and nanoparticle than that between particles of the same size.[12] The association between PLGA nanoparticles and PHEA-g-C_{18} microbubbles was evaluated by examining localization of fluorescently labeled nanoparticles on microbubbles and effects of nanoparticles on stability of microbubbles. The retention level of PLGA nanoparticles on the implanted tissue was assessed by examining sustained presence of particles on chicken chorioallantoic membranes (CAMs).[13] Finally, effects of nanoparticle retention on drug efficacy were studied by implanting PLGA nanoparticles encapsulating Angiopoietin-1 (Ang1) on CAMs and examining the degree of neovascularization.

2. RESULTS AND DISCUSSIONS

2.1 Preparation and characterization of polymeric microbubbles

Microbubbles were formed via self-assembly of amphiphilic polymer – PHEA grafted with octadecyl chains, termed PHEA-g-C_{18}. In the first step, polycondensation of $_{L}$-aspartic acid with acid catalyst led to polysuccinimide (PSI). Secondly, PSI was substituted with octadecylamine (ODA) and ethanolamine to form PHEA-g-C_{18} by aminolysis reactions

(Figure 1a).[14,15] With a molar ratio of ODA to succinimidyl units of PSI at 0.15, the degree of substitution for octadecyl chains (DS_{C18}) was 12.2 mol% as quantified with peaks from 0.80 to 0.86 ppm and peaks from 4.36 to 4.70 ppm in from ^{1}H NMR spectra (Figure S1). Note that peaks from 0.80 to 0.86 ppm represent protons of methyl groups at the end of the C_{18} chains and those from 4.36 to 4.70 ppm present methane protons on PHEA backbones.

In result, PHEA-g-C_{18} was able to self-assemble into microbubbles by sonication applied at the interface of air and polymer solution (Figure 1b). Particularly, microbubbles were assembled with polymer solutions at three different concentrations of the polymer to control size and stability (Figure 1c). Increasing concentration of polymer from 0.1% to 0.5% w/w decreased the average diameter of microbubbles from 194 ± 103 μm to 49 μm ± 36 μm, quantified with optical images. Further increasing the polymer concentration to 1% w/w made minimal change of the microbubble diameters; however, it contributed to improving the stability of bubbles incubated at 37 °C. Over 3 hours, the microbubbles prepared with 1% w/w polymer solution displayed a two-fold smaller increase in the diameter than those prepared with 0.5 % w/w polymer solution (Figure 1d).

This result suggested that sonication at air-water interface applies enough energy to drive hydrophobic association of octadecyl chains on PHEA with air molecules. Then, the polymers surround air molecules to reduce the thermodynamic free energy. Finally, hydroxyl groups on PHEA-g-C_{18} likely facilitate dispersion of microbubbles in aqueous media. Therefore, similar to a surfactant, increasing concentration of PHEA-g-C_{18} solution from 0.1% to 0.5% w/w should lead to an increase of the curvature of microbubbles. The minimal change of the microbubble size with an increase of polymer concentration from 0.5% to 1% w/w indicates that polymer association with air molecules is saturated at 0.5% w/w. The significantly enhanced microbubble stability marked by a smaller size change is likely because excess PHEA-g-C_{18} on the microbubble surface forming a steric layer prevents association between microbubbles and subsequent fusion.

2.2 Assembly of core-shell particles constituted with PLGA nanoparticles and PHEA-g-C_{18} microbubbles

Monodispersed PLGA nanoparticles with an average diameter of 100 nm were prepared via nanoprecipitation (Figure S2). Mixing aqueous suspension of PLGA nanoparticles with freshly made microbubbles resulted in microbubbles covered with PLGA nanoparticles (Figure 2a). According to the fluorescence image of PLGA nanoparticles labeled with fluorescein isothiocyanate (FITC), nanoparticles spontaneously adhered on microbubble surface, thus forming a core-shell like construct; in contrast, PLGA nanoparticles were randomly distributed in microbubble-free solution (Figure2b and 2c). Even after exposure to shear flow to simulate injection process, nanoparticles were minimally detached from the microbubbles, as confirmed with minimal decrease of fluorescence from the microbubble surface.

With assumption that interaction between two particles is minimally affected by neighboring ones, it is suggested that the association between microbubbles and nanoparticles are driven by van der Waals force calculated using Eq. (1):

$$V_A = -\frac{A}{6D}\frac{R_1 R_2}{R_1 + R_2} \quad \text{Eq. (1)}$$

where R_1 and R_2 are the radii of microbubbles and nanoparticles, respectively; A is the Hamaker constant; V_A is van der Waals potential energy; and D is the distance between two particles.[16] The Hamaker constants of PHEA and PLGA were considered 6.5×10^{-20} J.[12] The estimated attractive energy between PLGA nanoparticle and microbubble is about twice lower than that between PLGA nanoparticles (Table 1). According to the calculation, increasing a diameter of microbubbles from 10 to 200 μm does not alter the attractive energy much. It is conceived that the value of van der Waals potential depends on three-dimensional organization of particles in the suspension, which alters the value of Hamaker constant. However, it is likely that the difference of the interaction energy between the conditions examined herein will remain same because of the minimal difference of the spatial organization of particles.[17]

More interestingly, the core-shell particles remained stable in a physiologically relevant condition. At 37 °C, the microbubbles prepared with 1% w/w PHEA-g-C_{18} solution undertook a three-fold smaller increase of the diameter than bare microbubbles (Figure 2d). With the nanoparticle coating, the majority of microbubbles incubated in aqueous media for 3 hours was smaller than 50 μm, In contrast, the diameter of bare microbubbles ranged from 100 to 250 μm.

2.3 *In vivo* evaluation of PLGA nanoparticle retention

The core-shell particles in which PLGA nanoparticles were immobilized on PHEA-g-C_{18} microbubbles were placed on CAM, in order to evaluate an extent by which microbubbles improve the retention of PLGA nanoparticles on the implanted site. The PLGA nanoparticles were encapsulated with FITC, so as to monitor their spatial distribution on the CAM. Both two conditions underwent minimal displacement during the first 24 hours, as confirmed with small change of fluorescence yields (Figure3a and 3b).

However, between Day 1 and Day 7, fluorescence from free PLGA nanoparticles rapidly decreased. According to quantification of the fluorescence yield, approximately 90% of PLGA nanoparticles were displaced from the implanted site (Figure3a and 3b). The minimal displacement of PLGA nanoparticles during first 24 hours implicates that free PLGA nanoparticles could initially associate with CAM. However, the adhesion strength should be too weak to prevent the displacement over 7 days, because CAM undergoes continuous mechanical deformation due to an embryo's heart contraction. As a consequence, the PLGA nanoparticles should experience the increase of drifting velocity.[9]

Interestingly, in contrast, PLGA nanoparticles immobilized on microbubbles exhibited no significant decrease of fluorescence over 7 days. This result indicated that most of PLGA nanoparticles remained on the implanted site due to microbubbles (Figure3a and 3b). To confirm this theory, we implanted rhodamine B labeled PHEA-g-C_{18} microbubbles on CAMs over 7 days to analyze the behavior of polymeric microbubbles. According to

fluorescence image of PHEA-g-C_{18} microbubbles, approximately 80 % of PHEA-g-C_{18} molecules remained on the implanted site even after collapse (Figure 3c). Therefore, we suggest that PHEA-g-C_{18} in the collapsed microbubble hydrophobically associate with epithelium of CAM, while they still kept associating with PLGA nanoparticles (Figure 4). Overall, it is likely that PHEA-g-C_{18} microbubbles act as a glue for nanoparticles even after their structural collapse.

2.4 *In vivo* evaluation of neovascularization induced by Ang1-encapsulated PLGA nanoparticles

To demonstrate the importance of the retention of drug-releasing PLGA nanoparticles in improving therapeutic efficacy of drugs, PLGA nanoparticles were loaded with Ang1. Ang1 is known to stimulate angiogenesis by activating Tie2 receptors of endothelial progenitor and precursor cells. It is also known to play an important role in stabilizing endothelium of capillaries by recruiting pericytes.[18–20] In this study, the Ang1 molecules were loaded into the PLGA nanoparticles through nanoprecipitation. The efficacy of Ang1 to stimulating vascularization was evaluated by implanting these nanoparticles on CAM, which has been widely used for angiogenesis study.[13]

According to cross-sectional histological images stained for α-smooth muscle actin (α-SMA), the membranes implanted with Ang1-loaded PLGA nanoparticles presented about five-fold larger number of mature blood vessels than those treated with PBS (Figure 4a-I, 4a-II & 4b) Furthermore, CAM implanted with core-shell particles presented more than six-fold larger number of mature blood vessels than CAM implanted with free PLGA nanoparticles (Figure 4a–II & III & 4b). This enhanced neovascularization using the core-shell particles is well correlated to the retention level of PLGA nanoparticles on the implantation site. We interpret that free PLGA nanoparticles are displaced from the implanted site, thus reducing concentration of Ang1 on the implanted site. In contrast, PLGA nanoparticles immobilized on microbubbles stably remained at the implantation site and subsequently increased concentration of Ang1 on the implanted tissue. As a consequence, it is likely that Ang1 locally amplified cellular signaling involved with endothelial sprouting and pericyte recruitment.

To the best of our knowledge, we suggest that the result of this study is the first demonstration to improve nanoparticle retention on the implanted tissue without altering the surface chemistry or potential of nanoparticles or loading them in hydrogels. We believe that the results of this study will be useful to treat various tissue defects and pathologic tissues with low dosage of drug molecules and nanoparticles. In addition, the microbubbles would be useful as particulate glue to immobilizing a wide array of nanoparticles loaded with a series of growth factors and drug molecules. Furthermore, using the capability of microbubbles to create contrast of ultrasound images, the resulting system may enable us to conduct imaging-guided therapies.[21–23] Finally, the previous literature reported that PHEA based polymer presents minimal toxicity and is safe for in vivo study, and also particles made of PHEA-g-C18 have been extensively used as drug carriers injected in circulation.[15,24]

3. CONCLUSIONS

In conclusion, this study demonstrated that core-shell particles in which PLGA nanoparticles were immobilized on PHEA-g-C_{18} microbubble glue displayed enhanced retention on implanted tissue subject to dynamical mechanical loading. The association between nanoparticles and microbubbles resulted from simple mixing was driven by van der Waals attraction, due to the significant size difference. The nanoparticles loaded on the microbubbles stably remained on the implanted tissue over 7 days, likely because amphiphilic PHEA-g-C_{18} of the microbubbles could link nanoparticles to tissue even after collapse of microbubbles. Therefore, the core-shell particles encapsulated with Ang1 could stimulate formation of mature blood vessels, because of enhanced retention of particles and subsequently increased number of Ang1 on the implanted tissue. The results of this study will be useful to fully utilize advantages of a wide array of nanoparticles as drug carrier and improve quality of molecular therapies even with low dosage of drugs.

4. EXPERIMENTAL SESSION

4.1 Synthesis and characterization of PHEA-g-C_{18}

Poly(succinimide) (PSI, Mw 19,000 g/mol, PDI 1.5) was the starting chemical, synthesized through the acid-catalyzed polycondensation process of $_L$-aspartic acid (Sigma-Aldrich) described previously.[14] By aminolysis, PSI was functionalized with octadecylamine (ODA) (Sigma-Aldrich) and ethanolamine (Sigma-Aldrich) sequentially into PHEA-g-C_{18}.[15] PSI, dissolved in dimethylformamide, was reacted with the calculated amount of ODA at 70 °C for 24 hours. After the mixture was cooled down to the room temperature, the calculated amount of ethanolamine was added dropwise, and the reaction was continued for 6 hours. The final product was purified via dialysis against deionized (DI) water for 2 days followed by freeze-drying to obtain the dry powders. The structure of PHEA-g-C_{18} was characterized by ^{1}H NMR spectra, from which the degree of substitution of octadecyl chains (DS_{C18}) on the PHEA backbone was calculated.

4.2 Label PHEA-g-C18 with rhodamine B

50 mg of PHEA-g-C18 was dissolved in DI water along with 5 mg of rhodamine B (Sigma-Aldrich) for an overnight reaction whiling stirring. Then, the mixture was replaced into a dialysis bag for 1-day dialysis against DI water. The final powder product was collected by freeze-drying.

4.3 Assembly and characterization of PHEA-g-C_{18} microbubbles

Pre-microbubble solution was prepared by dissolving PHEA-g-C_{18} in DI water at concentrations of 0.1, 0.5, and 1% w/w. Then, the probe tip of a sonicator (Fischer Scientific, Sonic Dismembrator Model 100) was placed about 2 mm under the liquid surface, and the ultrasonic wave was applied with an average output power of 6 watts for 30 seconds, in order to generate a layer of microbubbles.

To analyze the size and stability of microbubbles, the microbubble solution was kept in 1.5 mL Eppendorf tube and incubated at 37 °C. Then, a 20 μL of microbubble solution was

collected from each sample at the time point of 0, 1, and 3 hours. The diameters of individual microbubbles visualized with an optical microscopy (Leica, DMIL) were measured using the ImageJ software.

4.4 Nanoprecipitation to prepare PLGA nanoparticles

PLGA nanoparticles were prepared via nanoprecipitation process, where 100 mg PLGA (Durect) dissolved in 10 mL acetone was added dropwise into 40 mL DI water. After precipitation, acetone was removed by using a rotary evaporator (Heidolph). Then, the PLGA nanoparticles in a powder form were collected via lyophilization. To prepare fluorescent PLGA nanoparticles, 0.1 mg fluorescein isothiocyanate (FITC) (Sigma-Aldrich) was dissolved in acetone together with PLGA.

Separately, the PLGA nanoparticles associated with Ang1 were prepared by dissolving Ang1 in 50 μL 1× phosphate buffered saline (1× PBS) at 5 μg/mL and mixing the Ang1 solution with the PLGA dissolved in acetone. Then, the mixture was added dropwise into 40 mL DI water. Finally, acetone was removed by using a rotary evaporator (Heidolph). The formed nanoparticles were washed with 1× PBS three times by centrifugation. Finally, the PLGA nanoparticles loaded with Ang1 was collected as powder via lyophilization.

4.5 Assembly and characterization of PLGA nanoparticle + PHEA-g-C_{18} microbubble core-shell particles

The microbubbles coated with PLGA nanoparticles were prepared by simply mixing aqueous suspension of microbubbles with PLGA nanoparticle suspension. The resulting morphology was observed with a laser scanning confocal microscope (Zeiss, LSM700). In this analysis, PLGA nanoparticles were labeled with FITC *in situ* as described in Section 4.3.

4.6 *In vivo* retention analysis of nanoparticles

Chick chorioallantoic membrane (CAM) was used to evaluate the retention level of the PLGA nanoparticles following implantation. PLGA nanoparticle + PHEA-g-C_{18} microbubble core-shell particles and free PLGA nanoparticles, which were not loaded on microbubbles, were separately placed onto the CAMs of one week old, fertilized chicken embryos. The particle suspension was gently dropped onto CAM surface by using a micropipette. PLGA nanoparticles in both conditions were labeled with FITC *in situ* described in Section 4.3. Then, the eggs were incubated at 37 °C. After time points of 1 hour, 1 day, and 7 days, CAMs at the implanted area were excised. The distribution of fluorescent PLGA nanoparticles on CAMs was identified by using a laser scanning confocal microscope (Zeiss, LSM700). The area covered with PLGA nanoparticles were quantified using a MATLAB code developed by the author.

4.7 *In vivo* neovascularization with Ang1-encapsulated PLGA nanoparticles

Ang1-encapsulated PLGA nanoparticle + PHEA-g-C_{18} microbubble core-shell particles and Ang1-encapsulated, free PLGA nanoparticles were implanted onto CAMs following the same procedure described in Section 4.5. After 7 days, CAMs at the implanted site were excised, embedded in paraffin, sectioned, and stained for antibody to α-smooth muscle actin

(α-SMA) for histological analysis. The number and area density of mature blood vessels marked by α-SMA were quantified with optical microscopy images (Leica, DMIL) of the cross-section of CAMs by using the Image J software.

4.8 Statistical analysis

All averaged data are presented as means ± standard deviation. To determine significance, comparisons between groups were performed by student's *t*-test ($p < 0.05$).

Supplementary Material

Refer to Web version on PubMed Central for supplementary material.

Acknowledgment

Work was funded by the National Institutes of Health (1R01 HL109192 to H.J.K. and R25 CA154015A to J.C.) and The Center for Advanced Study at the University of Illinois.

References

1. De Jong WH, Borm PJA. International Journal of Nanomedicine. 2008; 3(2):133–149. [PubMed: 18686775]
2. Wilczewska AZ, Niemirowicz K, Markiewicz KH, Car H. Pharmacological Reports. 2012; 64:1020–1037. [PubMed: 23238461]
3. Parveen S, Misra R, Sahoo SK. Nanomedicine: Nanotechnology, Biology and Medicine. 2012; 8(2): 147–166.
4. Kumari A, Yadav SK, Yadav SC. Colloids and Surface B: Biointerfaces. 2010; 75(1):1–18. [PubMed: 19782542]
5. Sun T, Zhang YS, Pang B, Hyun DC, Yang M, Xia Y. Angewadte Chemie International Edition. 2014; 53(46):12320–12364.
6. Li S-D, Huang L. Molecular Pharmaceutics. 2008; 5(4):496–504. [PubMed: 18611037]
7. Sa LTM, Albernaz MS, Patricio BFC, Junior MVF, Coelho BF, Bordim A, Almeida JC, Santos-Oliveira R. Journal of Pharmaceutical and Biomedical Analysis. 2012; 70:602–604. [PubMed: 22742922]
8. Kumar R, Roy I, Ohulchanskky TY, Vathy LA, Bergey EJ, Sajjad M, Prasad PN. ACS Nano. 2010; 4(2):699–708. [PubMed: 20088598]
9. Morgen M, Tung D, Boras B, Miller W, Malfait AM, Tortorella M. Pharm. Res. 2013; 30:257–268. [PubMed: 22996566]
10. DeVolder RJ, Kong HJ. Biomaterials. 2010; 31:6494–6501. [PubMed: 20538334]
11. Johnson C, Perlin L, Wyman P, Zhao B, Fullwood NJ, MacNeil S, Rimmer S. Macromolecular Symposia. 2010; 291–292:314–325.
12. Pierre, AC. Introduction to Sol-Gel Processing. 1st edn.. Massachusetts: Kluwer Academic Publishers; 1998.
13. Storgard C, Mikolon D, Stupack DG. Methods in Molecular Biology. 2005; 294:123–136. [PubMed: 15576910]
14. Tomida M, Nakato T, Matsunami S, Kakuchi T. Polymer. 1997; 38(18):4733–4736.
15. Kang H, Kim J-D, Han S-H, Chang I-S. Journal of Controlled Release. 2002; 81:135–144. [PubMed: 11992686]
16. Tadmor R. J. Phys.: Condens. Matter. 2001; 13:195–202.
17. Yannopapas V. Journal of Physical Chemistry C. 2013; 117(29):15342–15346.
18. Brindle NPJ, Saharinen P, Alitalo K. Circulation Research. 2006; 98:1014–1023. [PubMed: 16645151]

19. Cai J, Kehoe O, Smith GM, Hykin P, Boulton ME. Investigative Ophthalmology & Visual Science. 2008; 49(5):2163–2171. [PubMed: 18436850]
20. Khan AA, Paul A, Abbasi S, Prakash S. International Journal of Nanomedicine. 2011; 6:1069–1081. [PubMed: 21698074]
21. Stewart VR, Sidhu PS. The British Journal of Radiology. 2006; 79:188–194. [PubMed: 16498029]
22. Stride E, Edirisinghe M. Soft Matter. 2008; 4:2350–2359.
23. Wilson SR, Burns PN. Rodialogy. 2010; 257(1):24–39.
24. Mendichi R, Giammona G, Cavallaro G, Giacometti Schieroni A. Polymer. 2000; 41(24):8649–8657.

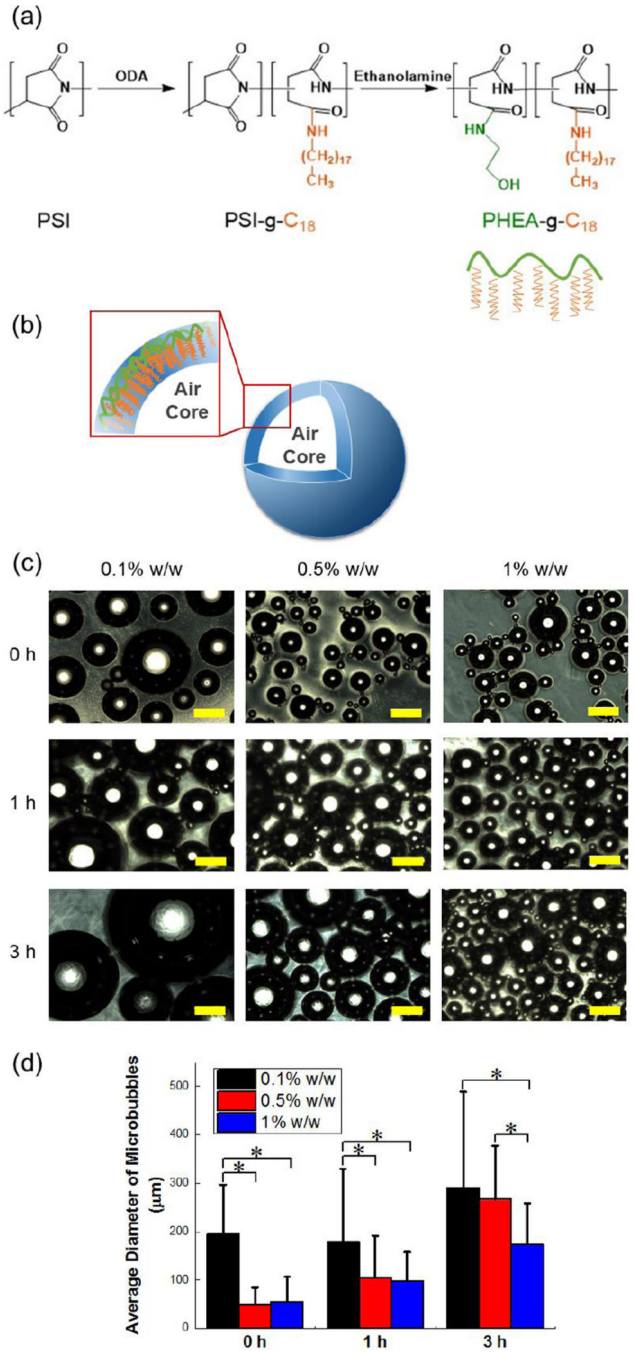

Figure 1.

Synthesis and characterization of PHEA-g-C_{18} microbubbles. (a) The reaction scheme to synthesize PHEA-g-C_{18}. (b) The schematic microstructure of the microbubble formed via self-assembly of PHEA-g-C_{18}. (c) Optical microscopy images of microbubbles prepared with solution of three different PHEA-g-C_{18} concentrations. The bubbles were captured at different time points while being incubated in deionized water at 37 °C. Scale bars represent 200 μm. (d) The size growth of microbubbles prepared with 0.1, 0.5, and 1% w/w PHEA-g-C_{18} solutions over 3 hours. The values and error bars in (d) represent average values and

standard deviation of more than 50 microbubbles per condition respectively. * represents the statistical significance of the values between conditions (* $p<0.05$).

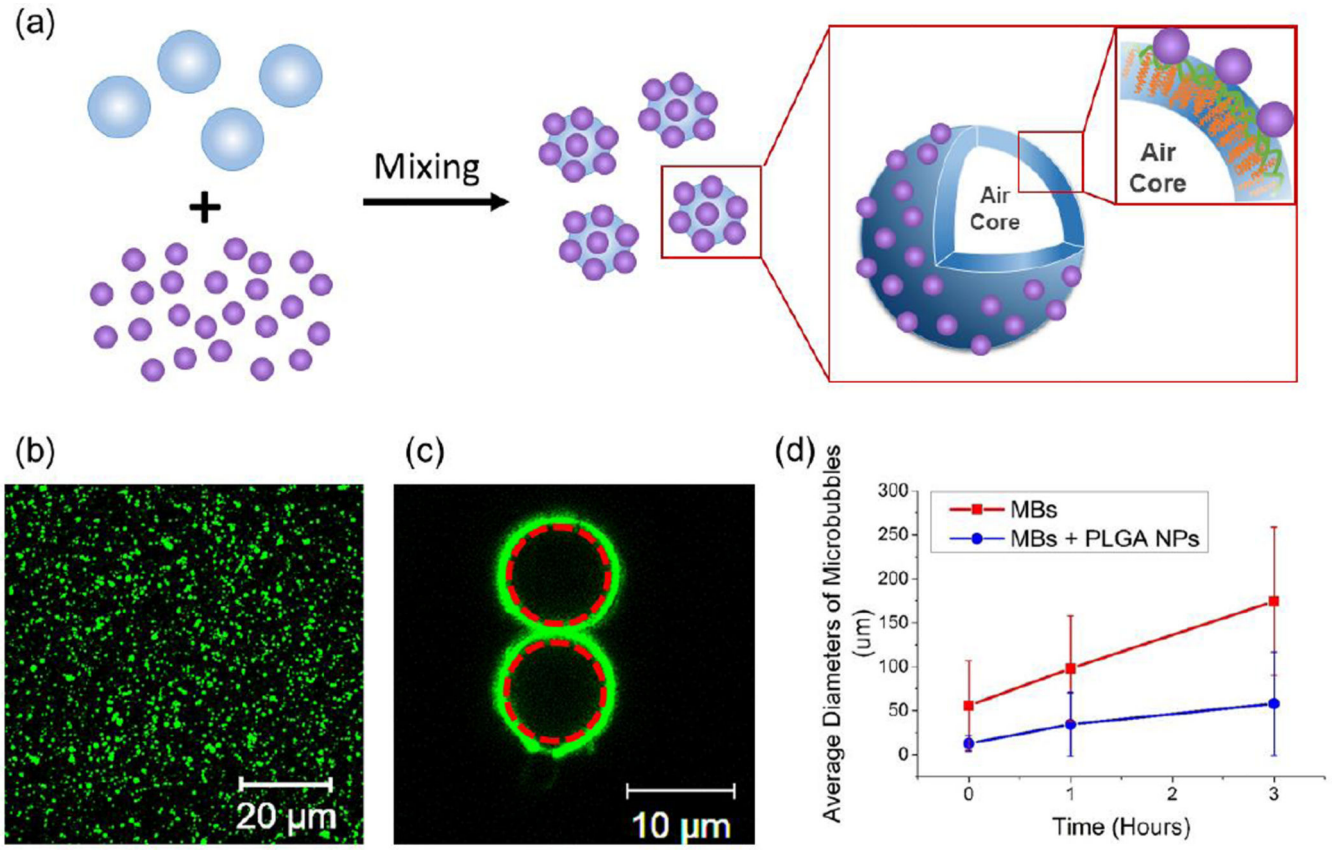

Figure 2.

Assembly of core-shell particles constructed with PLGA nanoparticles (NPs) and PHEA-g-C_{18} microbubbles (MBs). (a) The scheme to describe the microstructure of the core-shell particles. (b) The confocal microscopy image of FITC-labeled PLGA NPs. (c) The confocal microscopy image of PHEA-g-C_{18} MBs coated with FITC-labeled PLGA NPs. Red dotted circles represent the MBs. (d) The size growth of plain MBs, termed MBs, and MBs associated with PLGA NPs, termed MBs + PLGA NPs. MBs were prepared with 1% w/w PHEA-g-C_{18} solution. In (d), the values and error bars of each bar represent average values and standard deviation of more than 50 microbubbles per condition respectively.

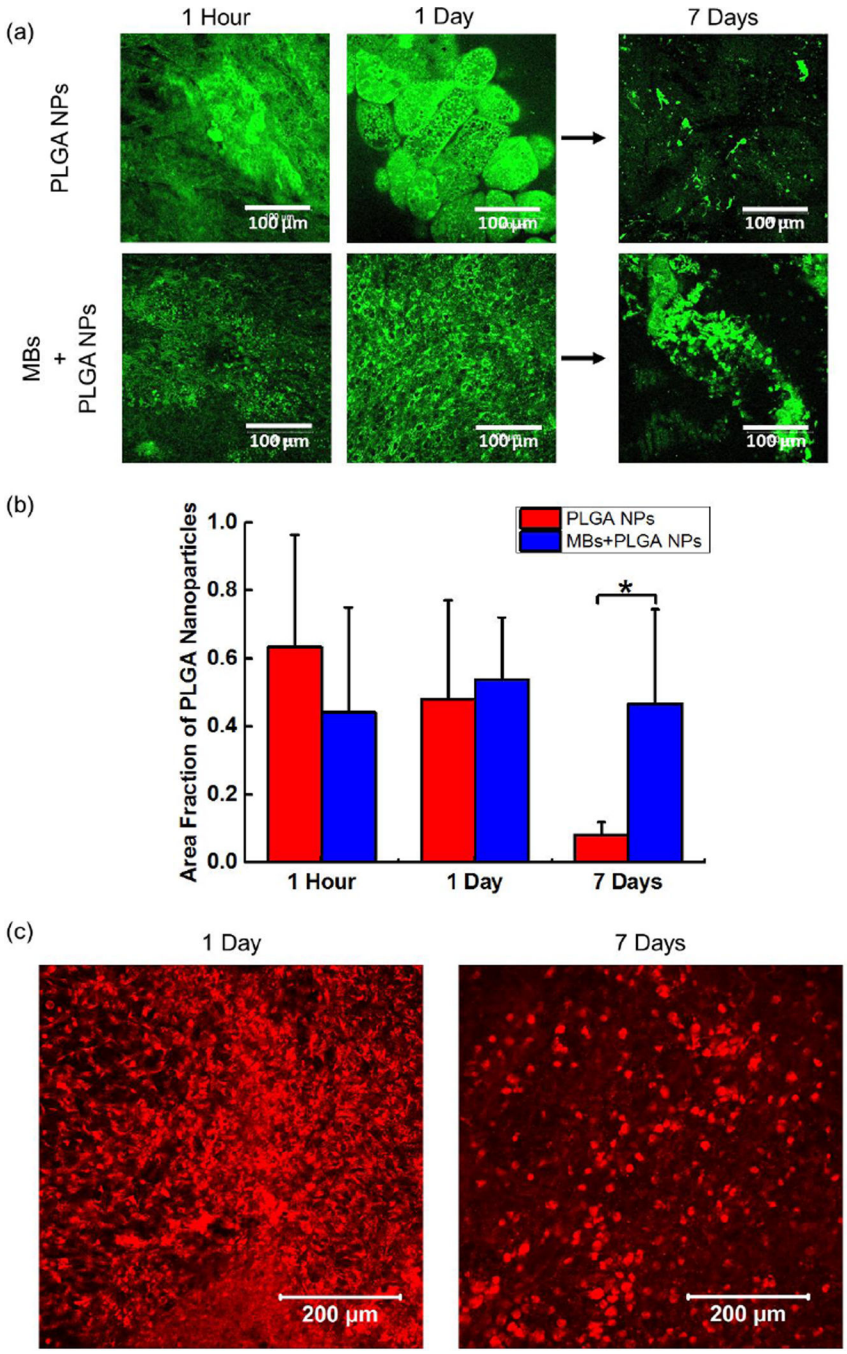

Figure 3.

In vivo evaluation of PLGA nanoparticle (NP) retention. (a) The confocal microscopy images of CAMs implanted with FITC-labeled PLGA NPs with and without microbubbles (MBs) at different time points. (b) The quantified fraction of PLGA NPs remained on the implantation site. The values and error bars represent average value and standard deviation of 9 samples per condition, respectively. (c) The confocal microscopy images of CAM implanted with rhodamine B labeled PHEA-g-C_{18} MBs at different time points. * represents the statistical significance of the values between conditions (* $p < 0.05$).

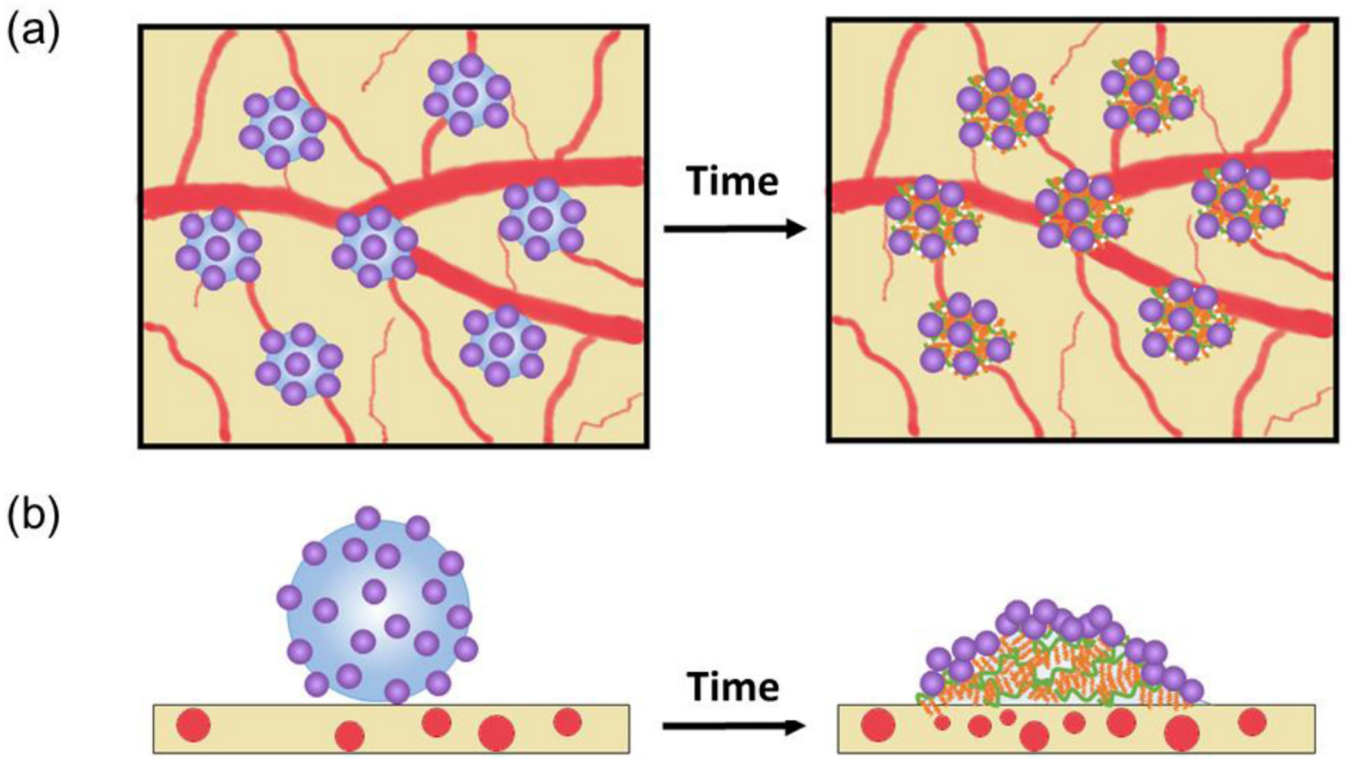

Figure 4.

The schematic description of the underlying mechanism by which PLGA nanoparticles coupled with microbubbles display minimal displacement over time. (a) and (b) represent top and side views of the core-shell particles on CAM respectively.

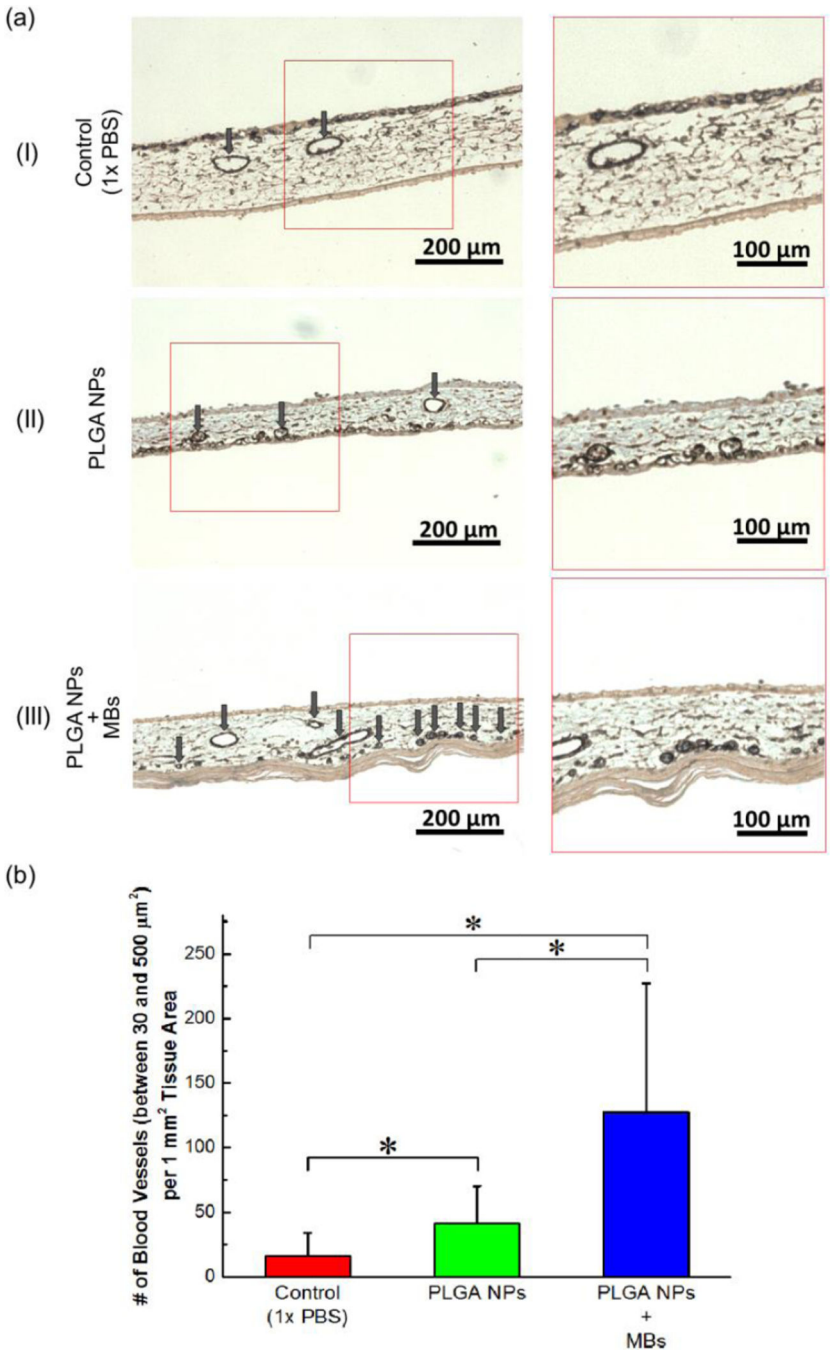

Figure 4.

In vivo evaluation of vascularization stimulated by Ang1-encapsulated PLGA nanoparticles (NPs). (a) Histological images of the cross session of CAMs stained for α-SMA. (a-I) CAM treated with PBS, (a-II) CAM treated with Ang1-encapsulated PLGA NPs, and (a-III) CAM treated with Ang1-encapsulated core-shell particles in which PLGA NPs were immobilized on the microbubbles (MBs). The images on the right column represent magnified views of the boxed region in the images on the left column. Arrows indicate mature blood vessels positively stained for α-SMA, marked by brown color. (b) Quantified number of mature

blood vessels with cross-sectional area between 30 and 500 μm^2 per tissue area of 1 mm^2. The values and error bars represent average values and standard deviation of 9 samples per condition. * represents the statistical significance of the values between conditions (* $p < 0.05$).

Table 1

Analysis of van der Waals potential for different particle interaction

	R_1 (μm)	R_2 (μm)	V_A (10^{-20} J)
Nanoparticle - Microbubble	0.05	5	−53.6
	0.05	50	−54.1
	0.05	100	−54.1
Nanoparticle - Nanoparticle	0.05	0.05	−27.1